Inorganica Chimica Acta 496 (2019) 119061

Contents lists available at ScienceDirect

Inorganica Chimica Acta

journal homepage: www.elsevier.com/locate/ica

Research paper

NHC-Ir(I) complexes derived from 5,6-dinitrobenzimidazole. Synthesis, characterization and preliminary evaluation of their *in vitro* anticancer activity

Arturo Sánchez-Mora[a], Hugo Valdés[a], María Teresa Ramírez-Apan[a], Antonio Nieto-Camacho[a], Simón Hernández-Ortega[a], Daniel Canseco-González[b], David Morales-Morales[a,*]

[a] Instituto de Química, Universidad Nacional Autónoma de México, Circuito Exterior, Ciudad Universitaria, Ciudad de México C.P. 04510, Mexico
[b] CONACYT-Laboratorio Nacional de Investigación y Servicio Agroalimentario y Forestal, Universidad Autónoma Chapingo, Texcoco de Mora, Mexico

ARTICLE INFO

Keywords:
Cancer
Cytotoxic activity
N-heterocyclic carbene
Iridium complexes
Fluorinated complexes
Antioxidant properties

ABSTRACT

The design, synthesis, characterization and *in vitro* anticancer activity of a series of Ir(I) NHC complexes derived from 5,6-dinitrobenzimidazole is reported. The evaluation was performed in five human cancer cell-lines, namely glioblastoma (U-251), prostatic adenocarcinoma (PC-3), colorectal adenocarcinoma (HCT-15), mammary adenocarcinoma (MCF-7) and lung adenocarcinoma (SKLU-7), including healthy cells of African green monkey kidney (COS-7) for comparative purposes. The complexes exhibited better activity in comparison with the corresponding NHC ligand precursors. In particular, complex (**4a**) exhibited a good performance against PC-3 and SKLU-1 with IC_{50} values of 10.6 ± 0.9 μM and 10.4 ± 1.5 μM, respectively.

1. Introduction

Cancer is one of the main causes of death around the world, producing 9.6 million deaths in 2018, only. Furthermore, each year there are 18.1 million new cases of cancer worldwide. Besides the incalculable human cost of cancer, its economical cost was estimated in $ 1.16 trillion USD. The estimation includes some important issues such as, treatment cost, productivity lost due to premature death and disability among others [1,2].

Patients with cancer are commonly treated with platinum derivatives, such as cisplatin, carboplatin and oxaliplatin [1–4]. In fact, nearly half of patients undergoing chemotherapy are treated with platinum drugs [5]. However, their use has been related to several side effects, such as infertility, alopecia, and anemia. In particular, cisplatin is also nephrotoxic and ototoxic [6,7]. In order to overcome these drawbacks, many research groups have focused their efforts on developing new potential anticancer compounds based on other transition metals, such as Au, Cu, Ru, Os, etcetera [8–26]. Recently, Ir has attracted much attention for the design of metallodrugs because of its antiproliferative and luminescent properties, especially when its oxidation state is + III [27–37]. However, there are only a few examples of Ir(I) complexes for this purpose [3,4,38–40]. Metzler-Nolte and co-workers described the cytotoxic activity of a series of complexes of the type [(NHC)IrCl(COD)] (Fig. 1), where NHC corresponds to a *N*-heterocyclic carbene ligand, more specifically they prepared the imidazolylidene and triazolylidene derivatives [41–43]. These compounds showed IC_{50} values in the micromolar scale, ranging from 10.3 ± 2.9 to 46.920 ± 0.085 μM for MCF-7.

In the past two decades, NHC ligands have become important motifs for the design of catalysts [44–46], as well as biological active compounds [8–26,47]. They form strong bonds with practically any transition metal, and can be easily prepared and functionalized, allowing the fine tuning of their electronic and steric properties. Based on the aforementioned reasons, herein we report the synthesis and cytotoxic activity of a series of Ir(I)–NHC complexes derived from 5,6-dinitrobenzimidazole (Fig. 1). The presence of the nitro groups at the NHC ligand may provide interesting biological properties to their related complexes. The nitro group can interact with biological nucleophiles such as proteins, amino acids, nucleic acids, and enzymes through non-covalent interactions and can be found in some antineoplasic, antibiotic, and antiparasitic agents [48,49]. Furthermore, the $-NO_2$ groups can be bioactivated by enzymatic reduction, producing reactive species that may serve as prodrugs, ultimately inducing the desired or undesired biological effects [48].

* Corresponding author.
E-mail address: damor@unam.mx (D. Morales-Morales).

https://doi.org/10.1016/j.ica.2019.119061
Received 19 May 2019; Received in revised form 22 July 2019; Accepted 8 August 2019
Available online 09 August 2019
0020-1693/

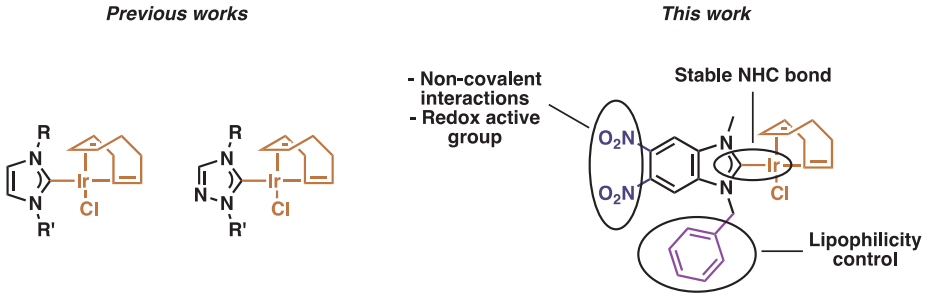

Fig. 1. Cytotoxic NHC-Ir(I) complexes.

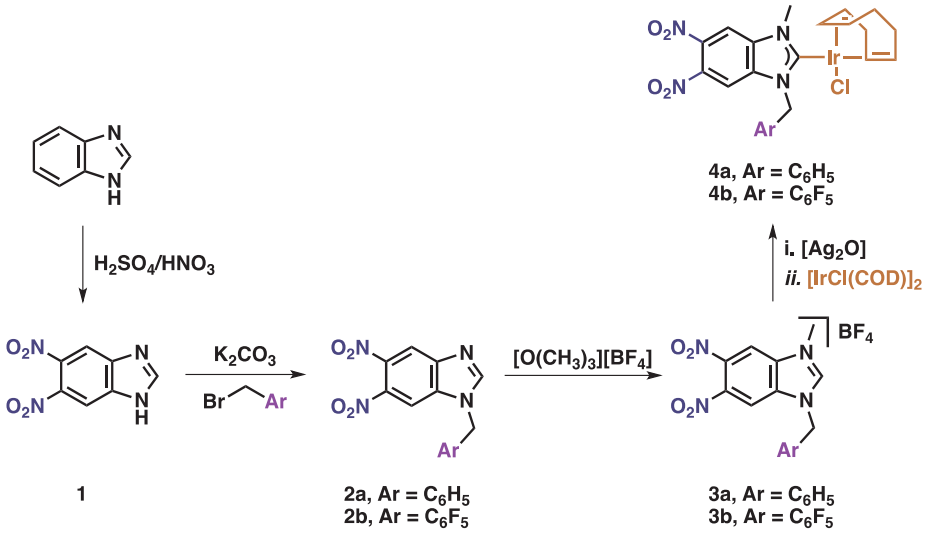

Scheme 1. Synthesis of 5,6-dinitrobenzimidazolium salts and Ir(I)–NHC complexes.

2. Results and discussion

2.1. Synthesis and characterization of NHC-Ir(I) complexes

The preparation of the 5,6-dinitrobenzimidazolium salts was performed in three steps from benzimidazole (Scheme 1). First, the nitration of benzimidazole was carried out using a mixture of H_2SO_4/HNO_3. The reaction was heated at 130 °C for 12 h. After purification 5,6-dinitro-1*H*-benzo[*d*]imidazole was isolated in a 52% yield. Afterwards, 5,6-dinitro-1*H*-benzo[*d*]imidazole was reacted with either benzyl bromide to afford (**2a**) (87%) or 2,3,4,5,6-pentafluorobenzyl bromide to afford (**2b**) (86%). In our study we chose two different *N*-substituent fragments, a benzyl and the fluorinated analog a pentafluorinated benzyl. The presence of fluorine atoms may increase the lipophilicity of the corresponding complex, and thus enhance its cytotoxic activity. Finally, compound (**2a**) or (**2b**) were reacted with trimethyloxonium tetrafluoroborate in 1,2-dichloroethane (Scheme 1). The 5,6-benzimidazolium salts (**3a**) and (**3b**) were obtained in 81% and 87% yield, respectively (Scheme 1).

All compounds were characterized by NMR spectroscopy, mass spectrometry and elemental analysis. The NMR spectra of the azolium salts (**3a**) and (**3b**) reveals a loss of symmetry. The most characteristic signal in the ^{1}H NMR spectra corresponds to the NC*H*N fragment at 10.06 and 10.14 ppm, respectively. In the $^{13}C\{^1H\}$ spectrum, the signals of the procarbenic carbon can be found at 150.2 ppm for (**3a**) and 150.4 ppm for (**3b**). The mass spectra of the azolium salts provide further information about their structures. The molecular ion $[M-BF_4]^+$ of (**3a**) and (**3b**) was observed at 313.10 and 403.22 *m/z*, respectively. All these data are in agreement with the proposed molecular structures.

The preparation of the Ir(I) complexes (**4a**) and (**4b**) was performed by a transmetallation reaction (Scheme 1). The reaction of Ag_2O with the corresponding azolium salt in acetonitrile, affords the Ag(I)–NHC derivatives (not isolated). Then, the addition of $[IrCl(COD)]_2$ to the solution produces the immediately precipitation of $AgBF_4$ and the formation of the desired product. The ^{1}H and $^{13}C\{^1H\}$ NMR spectra of the complexes were in agreement with the symmetry loss of the azolium salts. The most characteristic signal of the complexes corresponds to the metallated carbon that appears at 202.9 ppm. The mass spectra of the complexes were very clean, exhibiting peaks for the molecular ions at 648.0 *m/z* ($[M]^+$) for (**4a**) and 738.0 *m/z* ($[M]^+$) for (**4b**) respectively.

The molecular structure of complex (**4a**) was unequivocally determined by single crystal X-ray diffraction studies (Table 1, Fig. 2). Suitable crystals for this analysis were obtained by slow diffusion of hexane into a concentrated solution of the compound in 1,2-dichloroethane.

The structure reveals a distorted square planar geometry around the metal center. The NHC ligand is coordinated to Ir(I), one chlorine and one COD ligand complete the coordination sphere. The Ir(I)–NHC length is 2.004 (3) Å, being typical for this kind of compounds. As a consequence of the *trans* influence of the NHC ligand, the average distance of the carbons *trans* to the carbene carbon (2.19 (4) Å) is slightly longer than the distance of the carbons *trans* to the chlorine ligand (2.11 (4) Å). The crystal packing of (**4a**) showed two close contact interactions between pairs of molecules (Fig. 2), in which the nitro moieties are involved. The C(14)···O(2′) distance is 3.33 Å, while the C(7)···O(4′) bond distance is slightly longer, 3.41 Å.

2.2. Cytotoxic evaluation of Ir(I)–NHC complexes

Preliminary cytotoxic evaluation of all compounds was performed in five human cancer cell-lines; glioblastoma (U-251), prostatic

Table 1
Crystal data and structure refinement for (**4a**).

Empirical formula	$C_{23}H_{24}ClIrN_4O_4$
Formula weight	648.11
Temperature	298(2) K
Wavelength	0.71073 Å
Crystal system	Monoclinic
Space group	$P2_1/c$
Unit cell dimensions	a = 13.3172(5) Å α = 90° b = 14.3965(5) Å β = 96.7621(11)° c = 12.0061(4) Å γ = 90°
Volume	2285.81(14) Å^3
Z	4
Density (calculated)	1.883 Mg/m^3
Absorption coefficient	5.996 mm^{-1}
F(0 0 0)	1264
Crystal size	0.290 × 0.087 × 0.065 mm^3
Theta range for data collection	2.218–25.392°
Index ranges	$-16 \le h \le 12$, $-17 \le k \le 17$, $-14 \le l \le 14$
Reflections collected	17,262
Independent reflections	4201 [R(int) = 0.0227]
Completeness to theta = 25.242°	99.9%
Absorption correction	Semi-empirical from equivalents
Max. and min. transmission	0.7452 and 0.5065
Refinement method	Full-matrix least-squares on F^2
Data/restraints/parameters	4201/0/299
Goodness-of-fit on F^2	1.123
Final R indices [I > 2sigma(I)]	R1 = 0.0233, w$R2$ = 0.0449
R indices (all data)	R1 = 0.0280, w$R2$ = 0.0471
Largest diff. peak and hole	0.671 and − 0.447 e.Å^{-3}

adenocarcinoma (PC-3), colorectal adenocarcinoma (HCT-15), mammary adenocarcinoma (MCF-7) and lung adenocarcinoma (SKLU-1), as well as healthy cells of African green monkey kidney (COS-7) for comparative purpose. Tests were carried out using a single-dose of a 25 μM solution of the corresponding 5,6-dinitro compound derivative in DMSO. Table 2 shows the results of the evaluation. The azolium salts precursor (**2a**) was poorly active against all the cell lines, while compound (**2b**) inhibited the growth of PC-3 (30.5%) and SKLU-1 (52.7%) (Entry 2, Table 2). The only structural difference between (**2a**) and (**2b**) being the presence of the fluorinated aromatic ring in (**2b**). Thus, it is clear that the fluorine atoms play an important role in the behavior of this compound.

Regarding the azolium salts (**3a**) and (**3b**), their cytotoxic activity varies from 85.3% to 100%, being both more active than cisplatin (Entry 7, Table 2). However, both compounds (**3a**, 86.3%) and (**3b,** 98.3%) were very active also for COS-7. Interestingly, the coordination of Ir(I) decreased the inhibition of the growth of some tumor cell lines. Compound (**4a**) exhibited low inhibition for U-251 (25.3%) and HCT-15 (11.2%), while for PC-3, MCF-7 and SKLU-1 were very good, reaching a percentage of inhibition up to 100%. Fortunately, the percentage of inhibition growth for the healthy cell line COS-7 was low (7.9%). In contrast, the fluorinated complex (**4b**) was very active in all the evaluated cell lines, including COS-7.

Since compound (**4a**) exhibited low inhibition in healthy cells, we decided to determine its IC_{50} in two different human tumor cell lines. Thus, compound (**4a**) exhibited good cytotoxicity against PC-3 (10.6 ± 0.9 μM) and SKLU-1 (10.4 ± 1.5 μM), affording values in the micromolar scale. These values are similar to those found for cisplatin, 8.4 ± 0.8 μM for PC-3 and 4.3 ± 0.5 μM for SKLU-1, however with lower toxicity against healthy cells.

2.3. Antioxidant properties

The production of reactive Oxygen Species (ROS) is an important carcinogenic process through the promotion of cell proliferation-activating, growth-related signaling pathways [50]. Thus, given the relevance of this process and the fact that it may be possible that the complexes may engage in relevant redox processes we evaluated the antioxidant properties of both complexes (**4a**) and (**4b**), using the thiobarbituric acid reactive substances (TBARS) technique, which involves the production of ROS with $FeSO_4$ in the presence of lipids obtained from rat brain [51]. Finding that both species, do not produce ROS but possess antioxidant properties (Table 3).

For completeness the IC_{50} values for both complexes were also determined and compared with those of butylated hydroxytoluene (BHT) and α-tocopherol (Fig. 3) [52] two reference compounds with antioxidant properties.

3. Conclusions

In summary, we have synthesized and characterized a novel series of Ir(I)–NHC complexes derived from 5,6-dinitrobenzimidazole. The molecular structure of (**4a**) was unambiguously determined by single crystal X-ray diffraction analysis. The structure shows the NHC coordinated to Ir(I). The nitro groups favored H-bonds between pairs of molecules. On the other hand, the *in vitro* anticancer activity experiments showed that the presence of the fluorine atoms in the *N*-substituent increases the inhibition of the growth of human tumor cell lines, however, in some cases decreases the selectivity, inhibiting the growth of healthy cells (COS-7). The coordination of the NHC to IrCl (COD) favors the selectivity towards cancer cell lines compared with the NHC ligand precursor. Complex (**4a**) inhibited the growth of PC-3, MCF-7 and SKLU-7 in 99.0%, 100% and 68.7%, respectively, and was inactive for healthy cell (COS-7) representing the best case in this work. Furthermore, the IC_{50} values of (**4a**) for PC-3 and SKLU-7 were in the

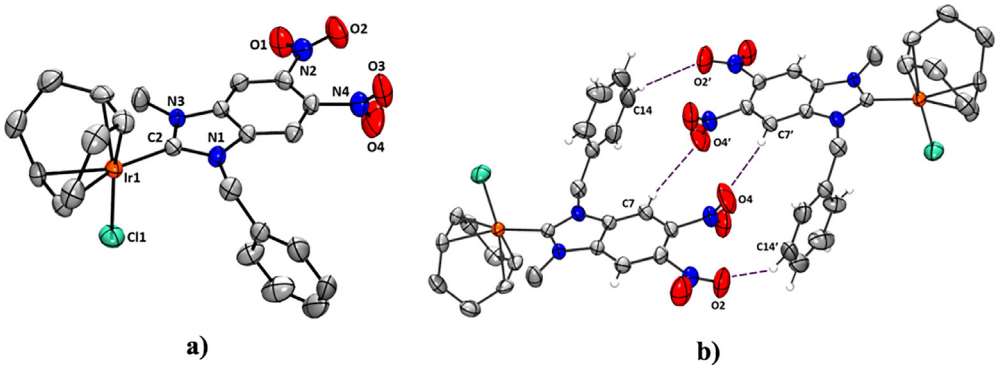

Fig. 2. a) Molecular structure of (**4a**). b) Close contact interactions between pairs of molecules. The ellipsoids are represented at 50% probability. Selected Bond Lengths (Å): Ir(1)-C(2) 2.004(3); Ir(1)-C(18) 2.107(3), Ir(1)-C(19) 2.111(4), Ir(1)-C(22) 2.184(4), Ir(1)-C(23) 2.204(4), Ir(1)-Cl(1) 2.3641(9), O(1)-N(2) 1.210(4), N(1)-C(2) 1.362(4), N(1)-C(11) 1.468(4), N(3)-C(2) 1.357(4), N(3)-C(10) 1.455(5), N(4)-O(4) 1.202(5), N(4)-O(3) 1.204(5), N(4)-C(6) 1.473(5), O(2)-N(2) 1.213(5), N(2)-C(5) 1.469(5). Selected Bond Angles (°): C(2)-Ir(1)-C(18) 89.12(14), C(2)-Ir(1)-C(19) 92.44(15), C(18)-Ir(1)-C(19) 39.35(15), C(2)-Ir(1)-C(22) 160.61(14), C(18)-Ir(1)-C(22) 96.70(15), C(19)-Ir(1)-C(22) 80.75(15), C(2)-Ir(1)-C(23) 162.20(14), C(18)-Ir(1)-C(23) 80.89(15), C(19)-Ir(1)-C(23) 89.13(15), C(22)-Ir(1)-C(23) 36.79(13), C(2)-Ir(1)-Cl(1) 90.98(10), C(18)-Ir(1)-Cl(1) 158.61(12), C(19)-Ir(1)-Cl(1) 161.85(12), C(22)-Ir(1)-Cl(1) 90.22(10), C(23)-Ir(1)-Cl(1) 93.03(11), O(4)-N(4)-O(3) 124.8(4), N(3)-C(2)-N(1) 105.7(3), N(3)-C(2)-Ir(1) 126.7(3), N(1)-C(2)-Ir(1) 127.5(3), O(1)-N(2)-O(2)124.3(4), C(19)-C(18)-Ir(1) 70.5(2), C(23)-C(22)-Ir(1) 72.4(2).

Table 2
Inhibition growth (%) of tumor cell lines at 25 μM by 5,6-dinitro compounds derivatives.

Entry		U-251	PC-3	HCT-15	MCF-7	SKLU-1	COS-7
1	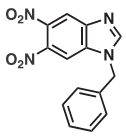 (**2a**)	6.8	10.5	–	6.4	0.2	2.1
2	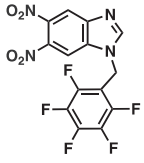 (**2b**)	–	30.5	6.6	–	52.7	1.1
3	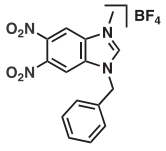 (**3a**)	100	85.3	100	100	100	86.3
4	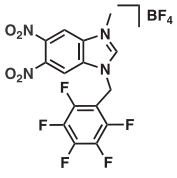 (**3b**)	100	100	100	92.7	100	98.3
5	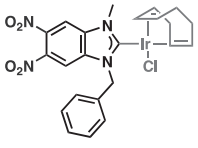 (**4a**)	25.3	99.0	11.2	100.0	68.7	7.9
6	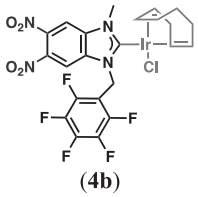 (**4b**)	75.0	100	100	100	99.0	93.2
7	Cisplatin	48.4	45.9	36.7	20.3	77.5	42.8

micromolar scale. Finally, the production of Reactive Oxygen Species (ROS) by complexes (**4a**) and (**4b**)was tested showing that both species do not produce ROS but instead have antioxidant properties even better than α-tocopherol, being (**4a**) the best in these assays. Consequently, this compound represents a good candidate to perform further studies, some of which are currently under developing in our laboratory.

4. Experimental

All chemical compounds were commercially obtained from Aldrich Chemical Co. and used as received without further purification. The ^{1}H and $^{13}C\{^{1}H\}$ NMR spectra were recorded on a Bruker Ascend 500 spectrometer. Chemical shifts are reported in ppm down field of TMS using the residual signals in the solvent as internal standard. Elemental analyses were performed on a Perkin Elmer 240. CHNS analyses were performed in Thermo Scientific Flash 2000 elemental analyzed, using a Mettler Toledo XP6 Automated-S Microbalance and sulfanilamide as standard (Thermo Scientific BN 217826, attained values N = 16.40%, C = 41.91%, H = 4.65% and S = 18.63%; certified values N = 16.26%, C = 41.81%, H = 4.71% and S = 18.62%). MS-Electrospray determinations were recorded on a Bruker Daltonics-Esquire 3000 plus Electrospray Mass Spectrometer. Melting points were carried out on Mel-Temp® Digital Melting Point Apparatus using open capillary tubes with a resolution of ± 1 °C.

4.1. Synthesis of 5,6-dinitro-1H-benzo[d]imidazole (1)

A solution of benzimidazole (12 g, 101.6 mmol) in H_2SO_4 (40 mL) was cooled at 0 °C in an ice bath. Then, fuming HNO_3 (80 mL) was added dropwise to the solution. The reaction was kept at 0 °C for 20 min more. After this time, it was slowly heated until a temperature of 130 °C was reached and was kept at this temperature for 12 h. After this time, the resulting reaction mixture was cooled at 0 °C and 200 g of ice were added. This solution was neutralized with NH_4OH, and the yellow solid obtained, filtered. This solid was purified by column chromatography using ethyl acetate as eluent, a pale-yellow band was separated. The resulting organic solution was concentrated until the precipitation of the desired product, which was then filtered. Yield: (52%). The

Table 3
Determination of Lipid peroxidation inhibition (rat brain).

Sample	Code	Concentration (μM)	TBARS (nmol/mg prot.)	Inhibition (%)	IC_{50} (μM)
4b (n = 3)	MMD5	Basal	0.273 ± 0.005		
		Control	8.305 ± 0.055		
		3	6.751 ± 0.099	18.7 ± 1.14	3.74 ± 0.12
		3.5	5.328 ± 0.592**	35.77 ± 7.39	
		4	2.171 ± 1.062**	73.7 ± 13.01	
		4.5	0.852 ± 0.251**	89.71 ± 3.1	
		5	0.665 ± 0.078**	91.98 ± 0.99	
		5.5	0.430 ± 0.028**	94.81 ± 0.37	
		6	0.402 ± 0.025**	95.16 ± 0.31	
4a (n = 3)	MMD6	Basal	0.273 ± 0.005		
		Control	8.305 ± 0.055		
		3	6.848 ± 0.068	17.54 ± 0.35	4.99 ± 0.19
		3.5	6.966 ± 0.233	16.09 ± 3.08	
		4	5.812 ± 0.238*	29.98 ± 3.31	
		4.5	5.511 ± 0.330*	33.59 ± 4.31	
		5	3.289 ± 1.034**	60.24 ± 12.63	
		5.5	2.512 ± 1.082**	69.58 ± 13.2	
		6	1.094 ± 0.435**	86.76 ± 5.35	
BHT (n = 3)		Basal	0.268 ± 0.053		
		Control	7.384 ± 0.630		
		0.56	6.098 ± 0.353	16.64 ± 2.86	1.22 ± 0.44
		0.75	5.559 ± 0.294*	23.92 ± 2.69*	
		1	4.457 ± 0.283**	37.14 ± 7.44**	
		1.33	3.228 ± 0.572**	53.59 ± 8.93**	
		1.78	1.315 ± 0.489**	81.59 ± 6.89**	
		2.37	0.487 ± 0.075**	93.16 ± 1.16**	
α-Tocopherol (n = 4)		Basal	0.200 ± 0.011		
		Control	6.589 ± 0.213		
		0.32	6.048 ± 0.242	8.26 ± 1.31	6.78 ± 2.16
		1	5.211 ± 0.332*	21.13 ± 2.56*	
		3.16	3.676 ± 0.569**	44.84 ± 6.74**	
		10	2.725 ± 0.335**	59.00 ± 3.71**	
		31.62	1.849 ± 0.319**	72.30 ± 3.87**	
		100	1.408 ± 0.364**	79.09 ± 4.79**	

Homogenized in: PBS; Vehicle: DMSO; Peroxidation: induce with $FeSO_4$ 10 μM, 1 h incubation; EDTA: 2 μM. The values are the average of three or four independent experiments ± standard error of the mean ($\bar{x} \pm ES$). Data were analyzed by one-way ANOVA followed by Dunnett's test for comparison against control. Values of $p \leq 0.05$ (*) and $p \leq 0.01$ (**) were considered statistically significant. The inhibitory concentration 50 (IC_{50}), was estimated by means of a linear regression.

spectroscopic data were similar to those reported in the literature [53].

4.2. General procedure for the synthesis of 1-substituted-5,6-dinitro-1H-benzo[d]imidazole

To a solution of 5,6-dinitro-1*H*-benzo[*d*]imidazole (1 eq.) and K_2CO_3 (1.5 eq.) in acetonitrile (100 mL) was added the corresponding benzyl bromide (1.2 eq.). The reaction was stirred and heated at 80 °C for 48 h. After this time, the resulting solution was cooled to room temperature and filtered through celite®. All the volatiles were removed under high vacuum and the crude product was washed several times with diethyl ether.

4.3. 1-benzyl-5,6-dinitro-1H-benzo[d]imidazole (2a)

For the synthesis of (**2a**), benzyl bromide (1.3 mL, 10.6 mmol), 5,6-dinitro-1*H*-benzo[*d*]imidazole (2.0 g, 9.6 mmol) and K_2CO_3 (1.9 g, 14.4 mmol) were used. Yield: 2.5 g (87%). ^{1}H NMR (500 MHz, $CDCl_3$) δ

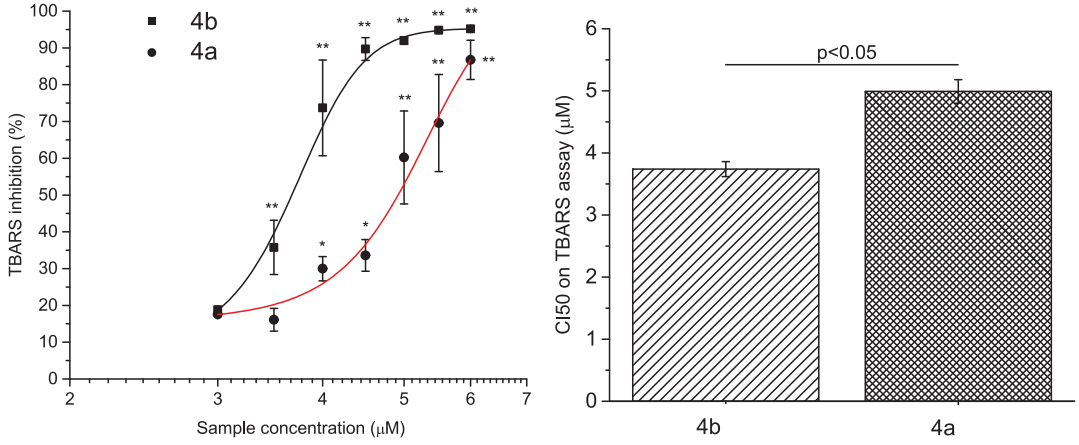

Fig. 3. IC_{50} values for complexes (**4a**) and (**4b**).

8.35 (s, 1H, CH_{BIm}), 8.28 (s, 1H, CH_{BIm}), 7.86 (s, 1H, CH_{BIm}), 7.43–7.40 (m, 3H, CH_{Ar}), 7.22–7.20 (m, 2H, CH_{Ar}), 5.46 (s, 2H, −CH_2−); $^{13}C\{^1H\}$ NMR (125 MHz, $CDCl_3$) δ 149.4 (NCHN), 145.1 (C_{BIm}), 139.8 (C_{BIm}), 139.7 (C_{BIm}), 134.8 (C_{BIm}), 133.3 (C_{Ar}), 129.8 (CH_{Ar}), 129.6 (CH_{Ar}), 127.4 (CH_{Ar}), 118.3 (CH_{BIm}), 108.4 (CH_{BIm}), 50.2 (−CH_2−). MS (EI^+): *m/z* 298 $[M]^+$. Elem. Anal. Calcd. for $C_{14}H_{10}N_4O_4$: C, 56.38; H, 3.38; N, 18.78. Found: C, 56.10; H, 3.35; N, 18.70. Melting Point: 173–174 °C.

4.4. 5,6-dinitro-1-((perfluorophenyl)methyl)-1H-benzo[d]imidazole (2b)

For the synthesis of (**2b**), 2,3,4,5,6-pentafluorobenzyl bromide (1.3 mL, 8.4 mmol), 5,6-dinitro-1*H*-benzo[*d*]imidazole (1.5 g, 7.2 mmol) and K_2CO_3 (1.49 g, 10.8 mmol) were used. Yield: 2.4 g (86%). ^1H NMR (500 MHz, DMSO-d_6) δ 8.83 (s, 1H, CH_{BIm}), 8.60 (s, 1H, CH_{BIm}), 8.59 (s, 1H, CH_{BIm}), 5.89 (s, 2H, −CH_2−). $^{13}C\{^1H\}$ NMR (126 MHz, DMSO-d_6) δ 151.2 (NCHN), 146.3–145.8 (m, CF_{Ar}), 144.2–144.1 (m, CF_{Ar}), 144.0 (C_{BIm}), 142.5–141.5 (m, CF_{Ar}), 140.3–139.6 (m, CF_{Ar}), 138.7 (C_{BIm}), 138.3 (C_{BIm}), 138.2–138.0 (m, CF_{Ar}), 136.7–135.7 (m, CF_{Ar}), 134.5 (C_{BIm}), 117.5 (CH_{BIm}), 109.7 (CH_{BIm}), 109.1 (t, $^3J_{C\text{-}F}$ = 17.4 Hz, C_{Ar}), 36.5 (−CH_2−). MS (EI^+): *m/z* 388 $[M]^+$. Elem. Anal. Calcd. for $C_{14}H_5F_5N_4O_4$: C, 43.31; H, 1.30; N, 14.43. Found: C, 43.69; H, 1.21; N, 14.44. Melting Point: 212–213 °C.

4.5. General procedure for the synthesis of azolium salts.

To a solution of (**2a**) or (**2b**) (1 eq.) in 1,2-dichloromethane (50 mL), trimethyloxonium tetrafluoroborate (1.6 eq) was added. The resulting solution was stirred at room temperature for 48 h and then cooled at 0 °C, to produce a solid that was filtered.

4.6. Azolium salt (3a)

For the synthesis of (**3a**), (**2a**) (1.2 g, 4.0 mmol) and trimethyloxonium tetrafluoroborate (1.0 g, 6.4 mmol) were used. Yield: 1.3 g (81%). ^1H NMR (500 MHz, Acetone-d_6) δ 10.06 (s, 1H, NC*H*N), 9.08 (s, 1H, CH_{BIm}), 8.98 (s, 1H, CH_{BIm}), 7.65 (m, 2H, CH_{Ar}), 7.48–7.46 (m, 3H, CH_{Ar}), 6.08 (s, 2H, −CH_2−), 4.46 (s, 3H, −CH_3). $^{13}C\{^1H\}$ NMR (125 MHz, Acetone-d_6) δ 150.2 (NCHN), 142.5 (C_{BIm}), 142.4 (C_{BIm}), 135.1 (C_{BIm}), 133.7 (C_{BIm}), 133.5 (C_{Ar}), 130.4 (CH_{Ar}), 130.3 (CH_{Ar}), 129.9 (CH_{Ar}), 114.1 (CH_{BIm}), 113.9 (CH_{BIm}), 52.7 (−CH_2−), 35.5 (−CH_3). MS (ESI^+): *m/z* 313.1 $[M-BF_4]^+$. Elem. Anal. Calcd. for $C_{15}H_{13}BF_4N_4O_4$: C, 45.03; H, 3.28; N, 14.00. Found: C, 44.94; H, 3.25; N, 13.94. Melting Point: 200–201 °C.

4.7. Azolium salt (3b)

For the synthesis of (**3b**), (**2b**) (1.0 g, 2.6 mmol) and trimethyloxonium tetrafluoroborate (0.6 g, 4.1 mmol) were used. Yield: 1.1 (87%). ^1H NMR (500 MHz, DMSO-d_6) δ 10.14 (s, 1H, NC*H*N), 9.20–9.18 (m, 2H, CH_{BIm}), 6.08 (s, 2H, −CH_2−), 4.15 (s, 3H, −CH_3). $^{13}C\{^1H\}$ NMR (125 MHz, DMSO-d_6) δ 150.5 (NCHN), 146.8–147.1 (m, CF_{Ar}), 144.9–145.1 (m, CF_{Ar}), 142.8–143.1 (m, CF_{Ar}), 141.1 (C_{BIm}), 140.9 (C_{BIm}), 138.3–138.7 (m, CF_{Ar}), 136.4–136.7 (m, CF_{Ar}), 133.7 (C_{BIm}), 132.5 (C_{BIm}), 113.9 (CH_{BIm}), 113.5 (CH_{BIm}), 107.7–107.3 (m, C_{Ar}), 39.0 (−CH_2−), 35.1 (−CH_3). MS (MALDI-TOF): *m/z* 403.22 $[M-BF_4]^+$. Elem. Anal. Calcd. for $C_{15}H_8BF_9N_4O_4$: C, 36.76; H, 1.65; N, 11.43. C, 36.86; H, 1.55; N, 11.41. Melting Point: 248–250 °C.

4.8. General procedure for the synthesis of the Ir(I)–NHC complexes

A solution of Ag_2O (0.5 eq) and the corresponding azolium salt (1 eq.) in acetonitrile (50 mL) was stirred under the exclusion of light at room temperature for 12 h. After this time $[IrCl(COD)]_2$ (0.5 eq) was added in one portion to the solution. The reaction was further stirred for 2 h. After this time, the solution was filtered through celite®. All the volatiles were removed under high vacuum and the crude product was purified by column chromatography. Elution with 1,2-dichloroethane affords a yellow band, which contains the desired product.

4.9. Complex (4a)

For the synthesis of (**4a**), Ag_2O (29 mg, 0.13 mmol), (**3a**) (100 mg, 0.25 mmol) and $[IrCl(COD)]_2$ (49 mg, 0.13 mmol) were used. Yield: 32.4 mg (20%). ^1H NMR (500 MHz, $CDCl_3$) δ 7.84 (s, 1H, CH_{BIm}), 7.43 (s, 1H, CH_{BIm}), 7.40–7.37 (m, 5H, CH_{Ar}), 6.36 (d, $^2J_{H\text{-}H}$ = 15.6 Hz, 1H, −CH_2−), 5.91 (d, $^2J_{H\text{-}H}$ = 15.6 Hz, 1H, −CH_2−), 4.96 (br s, 2H, CH_{COD}), 4.35 (s, 3H, −CH_3), 3.08–3.00 (m, 1H, CH_{COD}), 2.91–2–86 (m, 1H, CH_{COD}), 2.41–2.23 (m, 3H, C$H_{2\ COD}$), 2.19–2.09 (m, 1H, C$H_{2\ COD}$), 1.99–1.87 (m, 2H, C$H_{2\ COD}$), 1.87–1.78 (m, 1H, C$H_{2\ COD}$), 1.73–1.65 (m, 1H, C$H_{2\ COD}$). $^{13}C\{^1H\}$ NMR (125 MHz, $CDCl_3$) δ 202.9 (Ir-$C_{carbene}$), 139.1 (C_{BIm}), 138.9 (C_{BIm}), 136.8 (C_{BIm}), 135.5 (C_{BIm}), 133.7 (C_{Ar}), 129.5 (CH_{BIm}), 129.0 (CH_{BIm}), 127.4 (CH_{BIm}), 107.7 (CH_{BIm}), 106.4 (CH_{BIm}), 91.4 (CH_{COD}), 91.2 (CH_{COD}), 53.8 (CH_{COD}), 53.6 (CH_{COD}), 53.5 (−CH_2−), 35.4 (−CH_3), 33.7 (C$H_{2\ COD}$), 33.1 (C$H_{2\ COD}$), 29.4 (C$H_{2\ COD}$), 28.9 (C$H_{2\ COD}$). MS (FAB^+): *m/z* 648.0 $[M]^+$. Elem. Anal. Calcd. for $C_{23}H_{24}ClIrN_4O_4$: C, 42.62; H, 3.73; N, 8.64. Found: C, 42.80; H, 3.68; N, 8.63. Melting Point: 201–206 °C. SiO_2 TLC R_f (1,2-dicloroethane): 0.15

4.10. Complex (4b)

For the synthesis of (**4b**), Ag_2O (24 mg, 0.10 mmol), (**3b**) (100 mg, 0.20 mmol) and $[IrCl(COD)]_2$ (40 mg, 0.10 mmol) were used. Yield: 36.8 (24%). ^1H NMR (500 MHz, Acetone-d_6) δ 8.68 (s, 1H, CH_{BIm}), 8.46 (s, 1H, CH_{BIm}), 6.17 (d, $^2J_{H\text{-}H}$ = 16.0 Hz, 1H, −CH_2−), 5.99 (d, $^2J_{H\text{-}H}$ = 16.0 Hz, 1H, −CH_2−), 4.60–4.42 (m, 2H, CH_{COD}), 4.41 (s, 3H, −CH_3), 3.26–3.19 (m, 1H, CH_{COD}), 3.05–3.01 (m, 1H, CH_{COD}), 2.45–2.31 (m, 2H, C$H_{2\ COD}$), 2.30–2.21 (m, 1H, C$H_{2\ COD}$), 2.19–2.08 (m, 1H, C$H_{2\ COD}$), 2.01–1.92 (m, 1H, C$H_{2\ COD}$), 1.88–1.82 (m, 1H, C$H_{2\ COD}$), 1.73–1.65 (m, 1H, C$H_{2\ COD}$), 1.65–1.55 (m, 1H, C$H_{2\ COD}$). $^{13}C\{^1H\}$ NMR (125 MHz, Acetone-d_6) δ 202.9 (Ir-$C_{carbene}$), 147.0–146.8 (m, CF_{Ar}), 145.1–149.8 (m, CF_{Ar}), 142.5–142.1 (m, CF_{Ar}), 140.5–139.9 (m, CF_{Ar}), 139.1 (C_{BIm}), 138.9 (C_{BIm}), 138.9–138.5 (m, CF_{Ar}), 136.9 (C_{BIm}), 136.9–136.6 (m, CF_{Ar}), 136.1 (C_{BIm}), 111.–110.6 (m, C_{Ar}), 108.1 (CH_{BIm}), 107.9 (CH_{BIm}), 89.6 (CH_{COD}), 89.3 (CH_{COD}), 54.6 (CH_{COD}), 51.2 (CH_{COD}), 40.0 (−CH_2−), 35.6 (−CH_3), 34.3 (C$H_{2\ COD}$), 32.0 (C$H_{2\ COD}$), 29.3 (C$H_{2\ COD}$), 27.6 (C$H_{2\ COD}$). MS (FAB^+): *m/z* 738.0 $[M]^+$. Elem. Anal. Calcd. for $C_{23}H_{19}ClF_5IrN_4O_4$: C, 37.43; H, 2.59; N, 7.59. Found: C, 37.55; H, 2.57; N, 7.60. Melting Point: 223–227 °C. SiO_2 TLC R_f (1,2-dicloroethane): 0.15.

4.11. Cytotoxic evaluation

4.11.1. Cell lines culture and culture medium

The compounds were screened *in vitro* against human cancer cell lines: HCT-15 (human colorectal adenocarcinoma), MCF-7 (human mammary adenocarcinoma), U-251 (human glioblastoma), PC-3 (human prostatic adenocarcinoma), SKLU-1 (human lung adenocarcinoma), as well as COS-7 (healthy cells of African green monkey kidney). Cell lines were supplied by National Cancer Institute (USA). The human tumor cytotoxicity was determined using the protein-binding dye sulforhodamine B (SRB) in microculture assay to measure cell growth, as described in the protocols established by the NCI1.[54] The cell lines were cultured in RPMI-1640 medium supplemented with 10% fetal bovine serum, 2 mM L-glutamine, 10,000 units/mL penicillin G sodium, 10,000 l g/ml streptomycin sulfate and 25 μg/mL amphotericin B (Gibco) and 1% non-essential amino acids (Gibco). They were maintained at 37 °C in humidified atmosphere with 5% CO_2. The viability of the cells used in the experiments exceeds 95% as determined with trypan blue.

4.11.2. Cytotoxic assay

Cytotoxicity after treatment of the tumors cells and normal cell with

the test compounds was determined using the protein-binding dye sulforhodamine B (SRB) in microculture assay to measure cell growth [54]. The cells were removed from the tissue culture flasks by treatment with trypsin, and diluted with fresh media. Of this cell suspension, 100 μL containing 5000–10,000 cell per well, were pipetted into 96 well microtiter plates (Costar) and the material was incubated at 37 °C for 24 h in a 5% CO_2 atmosphere. Subsequently, 100 μL of a solution of the compound obtained by diluting the stocks were added to each well. The cultures were exposed for 48 h to the compound at concentrations 25 μM. After the incubation period, cells were fixed to the plastic substratum by addition of 50 μL of cold 50% aqueous trichloroacetic acid. The plates were incubated at 4 °C for 1 h, washed with tap H_2O, and air-dried. The trichloroacetic-acid-fixed cells were stained by the addition of 0.4% SRB. Free SRB solution was the removed by washing with 1% aqueous acetic acid. The plates were then air-dried, and the bound dye was solubilized by the addition of 10 mM unbuffered tris base (100 μL). The plates were placed on and shaken for 10 min, and the absorption was determined at 515 nm using a ELISA plates reader (Bio-Tex Instruments).

4.12. Lipid peroxidation inhibition

4.12.1. Animals

Adult male Wistar rat (200–250 g) was provided by the Instituto de Fisiología Celular, Universidad Nacional Autónoma de México (UNAM). Procedures and care of animals were conducted in conformity with Mexican Official Norm for Animal Care and Handling (NOM-062-ZOO-1999). They were maintained at 23 ± 2 °C on a 12/12 h light–dark cycle with free access to food and water.

4.12.2. Rat brain homogenate preparation

Animal sacrifice was carried out avoiding unnecessary pain. Ten rats were sacrificed with CO_2 to carry out all experiments. The cerebral tissue (whole brain), was rapidly dissected and homogenized in phosphate buffered saline (PBS) solution (0.2 g of KCl, 0.2 g of KH_2PO_4, 8 g of NaCl, and 2.16 g of $NaHPO_4{\cdot}7\ H_2O$/l, pH adjusted to 7.4) as reported elsewhere [55,56] to produce a 1/10 (w/v) homogenate. Then, the homogenate was centrifuged for 10 min at 800 rcf (relative centrifugal field) to yield a pellet that was discarded. The supernatant protein content was measured using the Folin and Ciocalteu's phenol reagent [57] and adjusted with PBS at 2.666 mg of protein/ml.

4.12.3. Induction of lipid peroxidation and thiobarbituric acid reactive substances (TBARS) quantification

As an index of lipid peroxidation, TBARS levels were measured using rat brain homogenates according to the method described by Ng et al. [58] with some modifications. Supernatant (375 μL) was added with 50 μL of 20 μM EDTA and 50 μL of each sample concentration solved in DMSO (50 μL of DMSO for control group) and incubated at 37 °C for 30 min. Lipid peroxidation was started adding 50 μL of freshly prepared 100 μM $FeSO_4$ solution (final concentration 10 μM) and incubated at 37 °C for 1 h. The TBARS content was determined as described by Ohkawa et al. [59] with some modifications. 500 μL of TBA reagent (1% 2-thiobarbituric acid in 0.05 N NaOH and 30% trichloroacetic acid, in 1:1 proportion) was added at each tube and the final suspension was cooled on ice for 10 min, centrifugated at 13,400 rcf for 5 min and heated at 80 °C in a water bath for 30 min. After cooling at room temperature, the absorbance of 200 μL of supernatant was measured at λ = 540 nm in a Bio-Tek Microplate Reader Synergy HT. Concentration of TBARS was calculated by interpolation in a standard curve of tetra-methoxypropane (TMP) as a precursor of MDA. Results were expressed as nmoles of TBARS per mg of protein. The inhibition ratio (I_R[%]) was calculated using following formula I_R = (C-E)*100/C, where C is the absorbance of control and E is the absorbance of the test sample. Butylated hydroxytoluene (BHT) and αtocopherol were used as positive standards.

All data were represented as mean ± standard error (SEM). Data were analyzed by one-way ANOVA followed by Dunnetís test for comparison against control. Values of $p \leq 0.05$ (*) and $p \leq 0.01$ (**) were considered statistically significant. The inhibitory concentration 50 (IC_{50}), was estimated by means of a linear regression.

4.13. Data collection and refinement for compounds 4a

A yellow and prism crystal of (**4a**), was grown from CH_2Cl_2/diethyl ether and mounted on glass fibers, then placed on a Bruker Smart Apex II diffractometer with a Mo-target X-ray source (λ = 0.71073 Å). The detector was placed at a distance of 5.0 cm from the crystal frames were collected with a scan width of 0.5 in ω and exposure time of 5 s/frame. 17,262 reflections were collected and integrated with the Bruker SAINT software package using a narrow-frame integration algorithm. Systematic absences and intensity statistics were used in monoclinic system and $P2_{1/c}$ space group. The structure was solved using Patterson methods using SHELXS-2014/7 program [60]. The remaining atoms were located via a few cycles of least squares refinements and difference Fourier maps. Hydrogen atoms were input at calculated positions and allowed to ride on the atoms to which they are attached. Thermal parameters were refined for all hydrogen atoms using a Ueq = 1.2 Å. The final cycle of refinement was carried out on all non-zero data using SHELXL-2014/7 [60]. Absorption correction was applied using SADABS program.

The crystallographic analysis was performed using PLATON [61] program, the figures of the molecular structures are represented using ellipsoids model while the supramolecular arrays were done using the ball and stick model, both representations were elaborate using the DIAMOND [62] program.

Acknowledgments

We would like to thank Chem. Eng. Luis Velasco Ibarra, Dr. Francisco Javier Pérez Flores, Q. Eréndira García Ríos, M.Sc. Lucia del Carmen Márquez Alonso, M.Sc. Lucero Ríos Ruiz, M.Sc. Alejandra Núñez Pineda (CCIQS), Q. María de la Paz Orta Pérez, Q. Roció Patiño-Maya and Ph.D. Nuria Esturau Escofet for technical assistance. H. V. would like to thank Programa de Becas Posdoctorales-DGAPA-UNAM for postdoctoral scholarships (Oficio: CJIC/CTIC/4751/2018). A. S.-M. would like to thank CONACYT (No. de becario: 629466) for M.Sc. scholarship. J.D.C-G would like to thank Programa de Cátedras CONACYT-PRY for generous support. The financial support of this research by PAPIIT-DGAPA-UNAM (PAPIIT IN207317) and CONACYT A1-S-33933 is gratefully acknowledged.

Appendix A. Supplementary data

Supplementary data for compound **4a** were deposited at the Cambridge Crystallographic Data Centre. Copies of this information are available free of charge on request from The Director, CCDC, 12 Union Road, Cambridge, CB2 1EZ, UK (Fax: +44-1223-336033; e-mail deposit@ccdc.cam.ac.uk or www: http://www.ccdc.cam.ac.uk) quoting the deposition numbers CCDC 1913480. Supplementary data to this article can be found online at https://doi.org/10.1016/j.ica.2019.119061.

References

[1] a) B. W. Stewart and C. P. Wild, Eds., World Cancer Report 2014, International Agency for Research on Cancer, Lyon, 2014.
[2] F. Bray, J. Ferlay, I. Soerjomataram, R.L. Siegel, L.A. Torre, A. Jemal, CA Cancer J. Clin. 68 (2018) 394–424.
[3] R.G. Kenny, C.J. Marmion, Chem. Rev. 119 (2018) 1058–1137.
[4] J.J. Wilson, S.J. Lippard, Chem. Rev. 114 (2014) 4470–4495.
[5] a) T.C. Johnstone, G.Y. Park, S.J. Lippard, Anticancer Res. 34 (2014) 471–476; b) A. Ramos-Espinosa, H. Valdés, M.T. Ramírez-Apan, S. Hernández-Ortega, B.A. Aguilar-Castillo, R. Reyes-Martínez, J.M. Germán-Acacio, D. Morales-Morales,

Inorg. Chim. Acta. 466 (2017) 584–590;
c) S. Ramírez-Rave, M.T. Ramírez-Apan, H. Tlahuext, D. Morales-Morales, R.A. Toscano, J.-M. Grévy, J. Organomet. Chem. 814 (2016) 16–24.
[6] A.M. Breglio, A.E. Rusheen, E.D. Shide, K.A. Fernandez, K.K. Spielbauer, K.M. McLachlin, M.D. Hall, L. Amable, L.L. Cunningham, Nat. Commun. 8 (2017) 1654.
[7] D.W. Shen, L.M. Pouliot, M.D. Hall, M.M. Gottesman, Pharmacol. Rev. 64 (2012) 706–721.
[8] S.M. Meier-Menches, C. Gerner, W. Berger, C.G. Hartinger, B.K. Keppler, Chem. Soc. Rev. 47 (2018) 909–928.
[9] L. Zeng, P. Gupta, Y. Chen, E. Wang, L. Ji, H. Chao, Z.-S. Chen, Chem. Soc. Rev. 46 (2017) 5771–5804.
[10] C.G. Hartinger, P.J. Dyson, Chem. Soc. Rev. 38 (2009) 391–401.
[11] C. Santini, M. Pellei, V. Gandin, M. Porchia, F. Tisato, C. Marzano, Chem. Rev. 114 (2014) 815–862.
[12] B. Englinger, C. Pirker, P. Heffeter, A. Terenzi, C.R. Kowol, B.K. Keppler, W. Berger, Chem. Rev. 119 (2019) 1519–1624.
[13] K.D. Mjos, C. Orvig, Chem. Rev. 114 (2014) 4540–4563.
[14] A. John, P. Ghosh, Dalton Trans. 39 (2010) 7183–7206.
[15] W. Liu, R. Gust, Chem. Soc. Rev. 42 (2013) 755–773.
[16] F. Hackenberg, M. Tacke, Dalton Trans. 43 (2014) 8144–8153.
[17] L. Oehninger, R. Rubbiani, I. Ott, Dalton Trans. 42 (2013) 3269–3284.
[18] G. Gasser, I. Ott, N. Metzler-Nolte, J. Med. Chem. 54 (2011) 3–25.
[19] G. Gasser, N. Metzler-Nolte, Curr. Opin. Chem. Biol. 16 (2012) 84–91.
[20] T. Zou, C.T. Lum, C.-N. Lok, W.-P. To, K.-H. Low, C.M. Che, Angew. Chem. Int. Ed. 53 (2014) 5810–5814.
[21] J. Lemke, A. Pinto, P. Niehoff, V. Vasylyeva, N. Metzler-Nolte, Dalton Trans. 107 (2009) 7063–7070.
[22] A. Gutiérrez, M.C. Gimeno, I. Marzo, N. Metzler-Nolte, Eur. J. Inorg. Chem. 2014 (2014) 2512–2519.
[23] R. Rubbiani, E. Schuh, A. Meyer, J. Lemke, J. Wimberg, N. Metzler-Nolte, F. Meyer, F. Mohr, I. Ott, Med. Chem. Commun. 4 (2013) 942–948.
[24] R. Rubbiani, I. Kitanovic, H. Alborzinia, S. Can, A. Kitanovic, L.A. Onambele, M. Stefanopoulou, Y. Geldmacher, W.S. Sheldrick, G. Wolber, A. Prokop, S. Wölfl, I. Ott, J. Med. Chem. 53 (2010) 8608–8618.
[25] W. Liu, R. Gust, Coor. Chem. Rev. 329 (2016) 191–213.
[26] P.O. Wagers, M.J. Panzner, M.R. Southerland, M.A. DeBord, M.C. Deblock, C.A. Tessier, C.L. Cannon, W.J. Youngs, Biologically Active N-Heterocyclic Carbene-Metal Complexes in *From Laboratory Curiosities to Efficient Synthetic Tools*, 2nd edn., Royal Society of Chemistry, Cambridge, 2016, pp. 567–595.
[27] K.K.-W. Lo, K.Y. Zhang, RSC Adv. 2 (2012) 12069–12083.
[28] Y. Geldmacher, M. Oleszak, W.S. Sheldrick, Inorg. Chim. Acta 393 (2012) 84–102.
[29] M. Graf, Y. Gothe, N. Metzler-Nolte, R. Czerwieniec, K. Sünkel, J. Organomet. Chem. 765 (2014) 46–52.
[30] C.-H. Leung, H.-J. Zhong, D.S.-H. Chan, D.-L. Ma, Coor. Chem. Rev. 257 (2013) 1764–1776.
[31] Z. Liu, P.J. Sadler, Acc. Chem. Res. 47 (2014) 1174–1185.
[32] Q. Du, L. Guo, M. Tian, X. Ge, Y. Yang, X. Jian, Z. Xu, Z. Tian, Z. Liu, Organometallics 37 (2018) 2880–2889.
[33] P. Štarha, Z. Trávníček, H. Crlíková, J. Vančo, J. Kasparkova, Z. Dvořák, Organometallics 37 (2018) 2749–2759.
[34] J. Li, M. Tian, Z. Tian, S. Zhang, C. Yan, C. Shao, Z. Liu, Inorg. Chem. 57 (2018) 1705–1716.
[35] A. Petrini, R. Pettinari, F. Marchetti, C. Pettinari, B. Therrien, A.N. Galindo, R. Scopelliti, T. Riedel, P.J. Dyson, Inorg. Chem. 56 (2017) 13600–13612.
[36] R.P. Paitandi, S. Mukhopadhyay, R.S. Singh, V. Sharma, S.M. Mobin, D.S. Pandey, Inorg. Chem. 56 (2017) 12232–12247.
[37] C.C. Konkankit, S.C. Marker, K.M. Knopf, J.J. Wilson, Dalton Trans. 47 (2018) 9934–9974.
[38] T. Giraldi, G. Sava, G. Mestroni, G. Zassinovich, D. Stolfa, Chem.-Biol. Interact. 22 (1978) 231–238.
[39] G. Sava, S. Zorzet, L. Paressin, Inorg. Chim. Acta 137 (1987) 69–71.
[40] E. Maftei, C.V. Maftei, P.G. Jones, M. Freytag, M.H. Franz, G. Kelter, H.-H. Fiebig, M. Tamm, I. Neda, Helv. Chim. Acta 99 (2016) 469–481.
[41] Y. Gothe, T. Marzo, L. Messori, N. Metzler-Nolte, Chem. Commun. 51 (2015) 3151–3153.
[42] Y. Gothe, T. Marzo, L. Messori, N. Metzler-Nolte, Chem. Eur. J. 22 (2016) 12487–12494.
[43] Y. Gothe, I. Romero-Canelón, T. Marzo, P.J. Sadler, L. Messori, N. Metzler-Nolte, Eur. J. Inorg. Chem. 2018 (2018) 2461–2470.
[44] E. Peris, Chem. Rev. 118 (2018) 9988–10031.
[45] M. Poyatos, J. Mata, E. Peris, Chem. Rev. 109 (2009) 3677–3707.
[46] J. Mata, M. Poyatos, E. Peris, Coor. Chem. Rev. 251 (2007) 841–859.
[47] a) J.M. Alfaro, A. Prades, M. del Carmen Ramos, E. Peris, J. Ripoll-Gómez, M. Poyatos, J.S. Burgos, Zebrafish 7 (2010) 13–21;
b) H. Valdes, D. Canseco-Gonzalez, J.M. German-Acacio, D. Morales-Morales, J. Organomet. Chem. 867 (2018) 51–54;
c) S. Ray, R. Mohan, J.K. Singh, M.K. Samantaray, M.M. Shaikh, D. Panda, P. Ghosh, J. Am. Chem. Soc. 129 (2007) 15042–15053;
d) L. Oehninger, R. Rubbiani, I. Ott, Dalton Trans. 42 (2013) 3269–3284;
e) J.L. Hickey, R.A. Ruhayel, P.J. Barnard, M.V. Baker, S.J. Berners-Price, A. Filipovska, J. Am. Chem. Soc. 130 (2008) 12570–12571;
f) A. Gautier, F. Cisnetti, Metallomics 4 (2012) 23–32.
[48] K. Nepali, H.-Y. Lee, J.-P. Liou, J. Med. Chem. (2018), https://doi.org/10.1021/acs.jmedchem.8b00147.
[49] M. Silva Lopes, C. Filizzola de Andrade Sena, B. Leonardo Silva, C. Maria de Souza, J. Pereira Ramos, G. Dantas Cassali, E. Maria de Souza-Fagundes, R. Jose Alves, M. Cristina de Oliveira, R. Barbosa de Oliveira, Anticancer Agents Med. Chem. 15 (2015) 206–216.
[50] S.J. Dixon, B.R. Stockwell, Nat. Chem. Biol. 10 (2014) 9–17.
[51] A. Lukaszewicz-Hussain, J. Moniuszko-Jakoniuk, J. Rogalska, Pol. J. Environ. Stud. 16 (2007) 233–236.
[52] T. Ohsima, V.V. Yankah, H. Ushio, C. Kiozumi, Adv. Exp. Med. Biol. 434 (1998) 181–188.
[53] K. Kincaid, J. Beckman, A. Zivkovic, R.L. Halcomb, J.W. Engels, R.D. Kuchta, Nucleic Acids Res. 33 (2005) 2620–2628.
[54] A. Monks, D. Scudiero, P. Skehan, R. Shoemaker, K. Paull, D. Vistica, C. Hose, J. Langley, P. Cronise, A. Vaigro-Wolff, M. Gray-Goodrich, H. Campbell, J. Mayo, M. Boyd, J. Natl. Cancer Ins. 83 (1991) 757–766.
[55] M. Dominguez, A. Nieto, J.C. Marin, A.S. Keck, E. Jeffery, C.L. Cespedes, J. Agric. Food Chem. 53 (2005) 5889–5895.
[56] J.I. Rossato, L.A. Ketzer, F.B. Centuriao, S.J. Silva, G. Lueni, A.L. Braga, M.A. Rubin, B.T. Rocha, Neurochem. Res. 27 (2002) 297–303.
[57] O.H. Lowry, N.J. Rosebrough, A.L. Farr, R.J. Randall, J. Biol. Chem. 193 (1951) 265–275.
[58] T.B. Ng, F. Liu, Z.T. Wang, Antioxidative activity of natural products from plants, Life Sci. 66 (2000) 709–723.
[59] H. Ohkawa, N. Ohishi, K. Yagi, Anal. Biochem. 95 (1979) 351–358.
[60] G.M. Sheldrick, Acta Cryst. C71 (2015) 3–8.
[61] A.L. Spek, Acta. Crystallogr. D65 (2009) 148–155.
[62] K. Brandenburg, M. Berndt, J. Appl. Cryst. 32 (1999) 1028–1029.